J Mol Model (2006) 12: 953–963
DOI 10.1007/s00894-005-0055-1

ORIGINAL PAPER

Olaf G. Othersen · Harald Lanig · Timothy Clark

The structure of 5a,6–anhydrotetracycline and its Mg^{2+} complexes in aqueous solution

Received: 6 July 2005 / Accepted: 23 September 2005 / Published online: 3 May 2006

Abstract Semiempirical molecular orbital theory has been used for a systematic scan of the binding positions for a Mg^{2+} ion with 5a,6–anhydrotetracycline taking both conformational flexibility and possible different tautomeric forms into account. The magnesium ion has been calculated alone and with four or five complexed water molecules in order to simulate the experimental situation more closely. The results are analyzed by comparing the behavior of the title compound with that of tetracycline itself and possible causes for the stronger induction of the Tetracycline Receptor (TetR) by 5a,6–anhydrotetracycline than by tetracycline are considered.

Keywords AM1 · 5a,6–anhydrotetracycline · Conformational analysis · Magnesium interactions

Introduction

The tetracycline class of antibiotics [1] has recently gained increased significance because of its ability to induce expression of the tetracycline repressor (TetR) and tetracycline antiporter (TetA) proteins as part of the resistance mechanism evolved to remove tetracyclines actively from bacterial cells [2]. This system has become an important tool that allows gene expression to be turned on and off at will with tetracyclines [3]. 5a,6–anhydrotetracycline, **1**, a toxic photoproduct from tetracycline, [4] although a weaker antibiotic than tetracycline, **2**, is found to be approximately 500 times more effective in inducing the expression of TetR and TetA by complexing to the dimeric TetR protein [5]. **1** is also notable for its ability to induce TetR without dipositive metal ions, which are essential for induction with other tetracyclines [6]. Thus, the efficiency of **1** as an inducer when complexed to Mg^{2+}, the metal ion usually involved in TetR induction, and its ability to induce in the absence of metal ions make it an attractive compound for research into the induction mechanism of the TetR system. Unfortunately, the structure of **1** in aqueous solution is hardly less complicated than that of tetracycline, **2**, especially in the presence of metal ions.

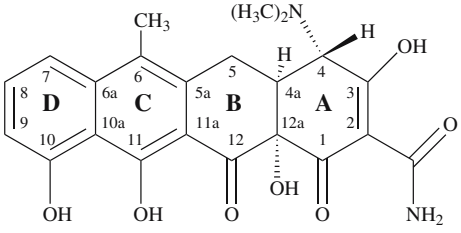

2 is known both experimentally [7] and from theoretical studies [8, 9] to exist in two distinct conformations, designated *extended* and *twisted*. The *extended* conformation is found to be the more stable in aqueous solution, although the more compact *twisted* structure is calculated to be more stable in the gas phase [9, 10]. Furthermore, nine different tautomers of neutral **2** were found to lie within 5 kcal mol^{-1} of the most stable structure at 298 K in aqueous solution [9, 10]. Complexation to Mg^{2+} was found computationally not to affect the relative stabilities of the *twisted* and *extended* conformations of tetracycline significantly, but to have a major effect on the tautomeric equilibria [11].

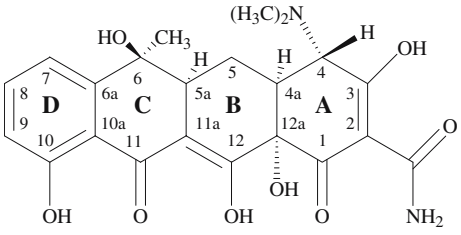

Electronic Supplementary Material Supplementary material is available for this article at http://dx.doi.org/10.1007/s00894-005-0055-1

O. G. Othersen · H. Lanig · T. Clark (✉)
Computer-Chemie-Centrum,
Friedrich-Alexander-Universität Erlangen-Nürnberg,
Nägelsbachstraße 25,
91052 Erlangen, Germany
e-mail: clark@chemie.uni-erlangen.de

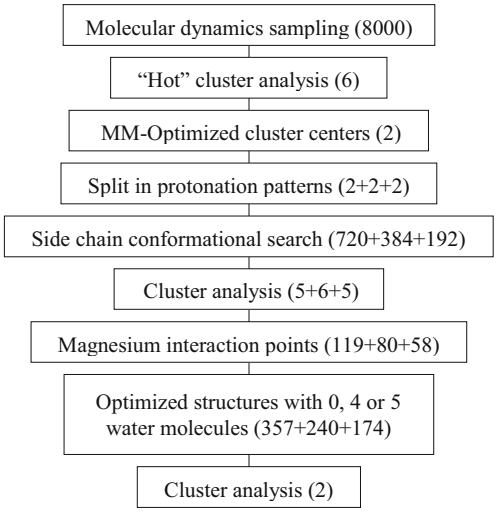

Scheme 1 Flow chart of the scan procedure. The numbers of structures obtained in each step are given in *brackets*. Triple entries indicate the different numbers for **1n**, **1z** and **1a**, respectively

1 is also known [12] to exist in *extended* and *twisted* conformations. Less flexibility than in **2** might be expected because of the extra quinone-like (B) ring, which could explain its stronger binding to the TetR dimer because of less loss of conformational entropy on binding. We now report an extensive study of the conformations of three protonation states of **1** and their complexes with hydrated magnesium ions analogous to our previous work [8, 11] on tetracycline. Note that an extensive conformational study on a series of tetracyclines has appeared recently [13]. This work is intended as a high-volume scan of the conformational and tautomeric diversity, rather than a definitive high-level computational study of relative stabilities. Semiempirical molecular orbital techniques are well suited for such purposes, whereas force-field methods have shown significant deficiencies for related problems [14]. As for tetracycline, [11] the results of this work will be used for high-level (density functional theory, DFT) studies on the structures and tautomers of **1** in aqueous solution.

Materials and methods

The different protonation states used for 5a,6–anhydrotetracycline are shown below. The labeling of the rings and atoms given above will be used throughout. Two neutral structures, the completely unionized tautomer **1n** and the commonly accepted zwitterion **1z**, and the anionic zwitterionic structure **1a** were considered.

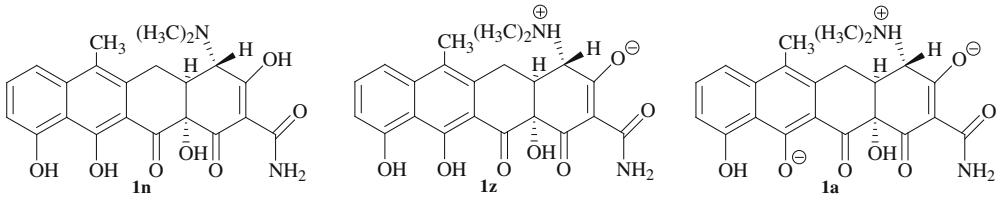

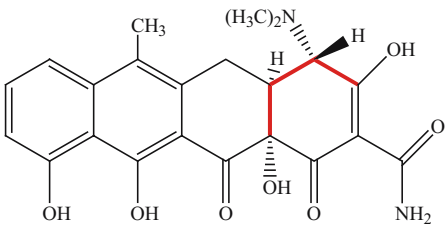

3-4-4a-12a

Cluster	Dihedral Angle (°)		
	3-4-4a-12a	4a-5-5a-6	1-12a-4a-5
1	-41.0	-176.7	-66.0
2	23.0	157.1	-174.6
3	-1.6	136.8	-162.6
4	36.9	175.3	167.3
5	40.9	153.8	-171.8
6	-40.4	-146.8	-76.6

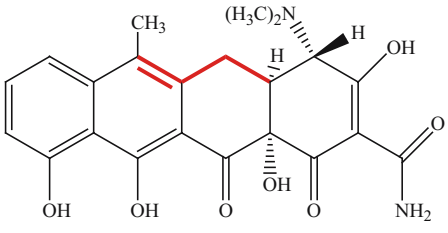

4a-5-5a-6

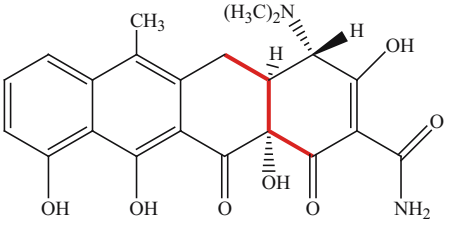

1-12a-4a-5

Scheme 2 Location and values of selected dihedral angles for the "hot" cluster centers from the molecular-dynamics simulation

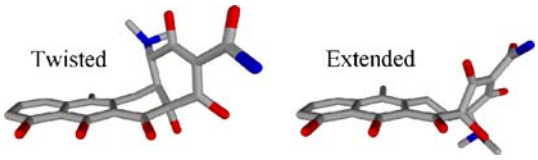

Scheme 3 Representative structure examples of **1** for the *twisted* and *extended* conformations. Hydrogen atoms are omitted throughout for clarity

All molecular mechanics calculations were performed with AMBER 5.0 [15] using the parm94 force field [16]. The semiempirical calculations used VAMP 9.0 [17] with the AM1 Hamiltonian [18] using the magnesium parameters published by Hutter et al. [19] For the consideration of solvent influence COSMO [20] was used. Cluster analyses were performed with TSAR 3.3 [21] using Ward's procedure [22].

8,000 initial conformations of **1** in its unionized form, generated by molecular dynamics simulations at a constant temperature of 1,200 K, heat-bath coupling constant of 2.0 ps, constant dielectric scaling constant of 4.0, a time-step of 0.5 fs, a time of 50 fs between snapshots and no cutoffs, were clustered by their ring conformation into six different structures. Time-dependent data for 31 dihedral angles were extracted from the molecular dynamics trajectory file. Angles

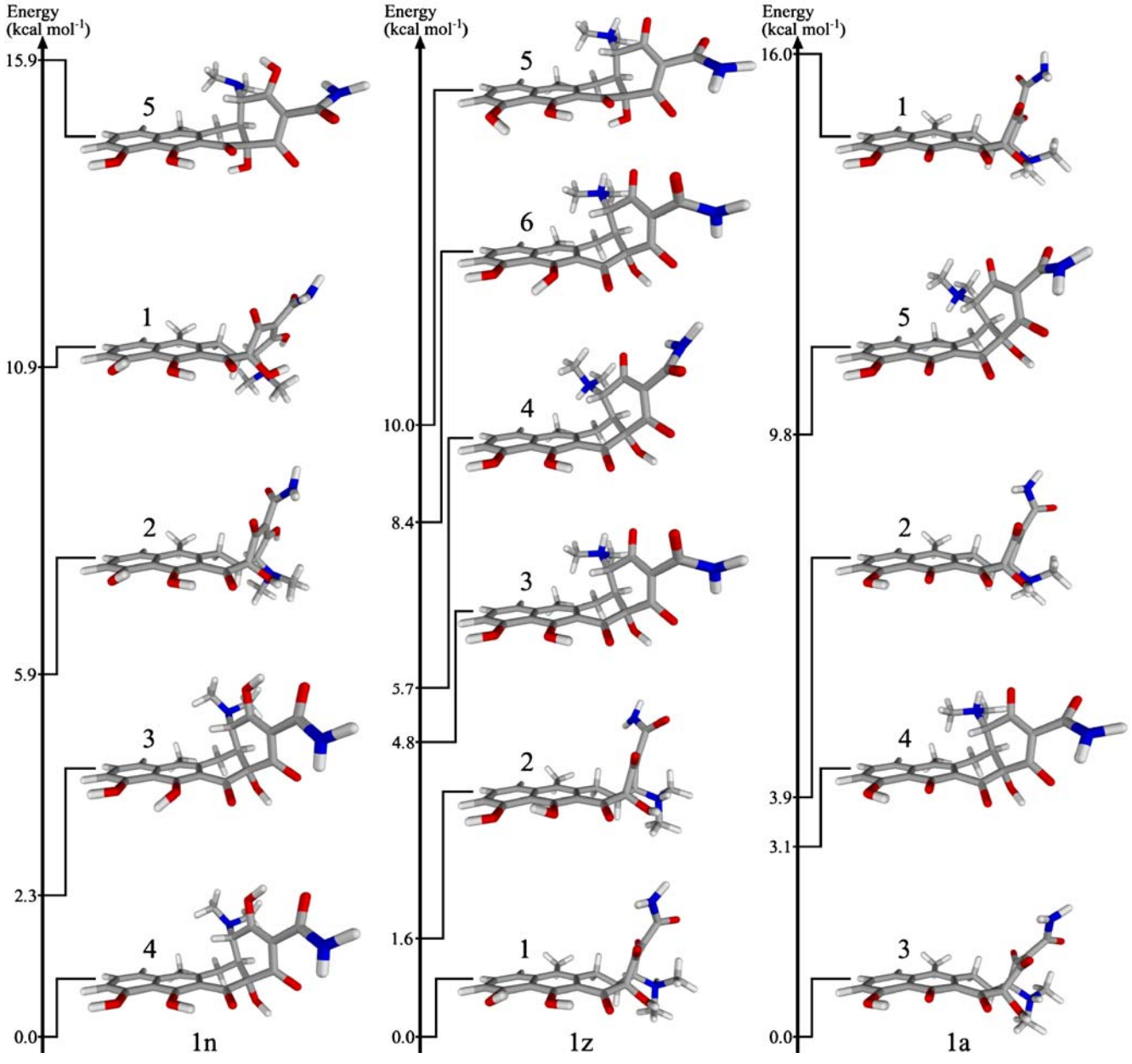

Fig. 1 Conformations and energy differences in the gas phase for **1n**, **1z**, and **1a**. The numbers indicate the different conformations and are consistent for Table 1, and Figs. 1, 2 and 3

with the highest information content in describing conformational changes were selected and highly correlated angles were removed for clustering. After molecular mechanics (MM) optimization and removal of converged structures, the minimized cluster centers were used to create zwitterionic and zwitteranionic protonation states for each conformation. The transfer of the O_3 hydrogen to N_{amine} generated **1z** and **1a**. Additionally, O_{12} was deprotonated to generate the protonation state **1a**. Systematic conformational searches for all polar and rotatable side chains were carried out in the gas phase using AM1 with full geometry optimization for all three conformations of the three protonation states. The resulting geometries for each protonation pattern were again clustered by their ring geometries. The clustering technique used is described in detail in [8].

The resulting cluster centers were reoptimized with AM1, but this time including a solvent correction for water using COSMO. The resulting structures were all used for systematic scans of interaction positions with a magnesium ion. Special regard was paid to interaction positions masked by acidic hydrogen atoms. The structures thus obtained for significant magnesium positions were fully optimized with AM1/COSMO. Alternate water complexation spheres for the metal ion containing either four or five water molecules were generated for each significant magnesium position and also fully optimized with AM1/COSMO. Details of the scan procedure can be found in [11].

As optimization of a sample of structures calculated to have low imaginary frequencies did not result in significant changes in geometry and heat of formation, low imaginary frequencies were ignored. Finally, the conformational similarities to the X-ray structure of tetracycline in the binding site of TetR (pdb–entry: 2TRT [23]), the intramolecular hydrogen bond networks and the Boltzmann populations in water at 298 K, using the absolute minimum for each total formula as reference, were calculated. Geometries were superimposed according to the root-mean–square deviation (RMSD) of their heavy-atom positions using Quatfit [24]. The exact sequence of the calculations performed and the number of structures resulting from each step is shown as a flow chart in Scheme 1.

Results

Metal-free 5a,6–anhydrotetracycline

Scheme 2 shows the conformationally descriptive dihedral angles 3-4-4a-12a, 4a-5-5a-6 and 1-12a-4a-5 for the six "hot" clusters of the molecular dynamics simulation. Angles and their boundaries used for the clustering of the trajectory structures are given in Table S1 of the supplementary material. The six different "hot" cluster centers converge to the *twisted* **T** or *extended* **E** conformations (Scheme 3) known in literature [7] and were used to generate the zwitterionic **1z** and zwitteranionic form **1a**.

Systematic conformational searches for polar and rotatable bonds of the side chains resulted in six clusters for **1z** and five clusters each for **1n** and **1a**, as shown in Fig. 1. Their heats of formation and conformationally descriptive dihedral angles are shown in Table 1. The absolute minimum of **1n** is conformation **T**, with an energy difference of 5.9 kcal mol^{-1} to **E**, whereas **1z** and **1a** prefer conformation **E** over **T** by 4.8 and 3.1 kcal mol^{-1}, respectively. Within **T** and **E** the conformations differ

Table 1 Heat of formation (AM1) and selected dihedral angles for the different gas phase and COSMO optimized conformations of **1n**, **1z** and **1a**

Protonation state	Conformation	Gas phase optimized				COSMO optimized			
		ΔH_f^0 (kcal mol^{-1})	Dihedral angles (°)			ΔH_f^0 (kcal mol^{-1})	Dihedral angles (°)		
			3-4-4a-12a	4a-5-5a-6	1-12a-4a-5		3-4-4a-12a	4a-5-5a-6	1-12a-4a-5
1n	1	−205.2	−26.7	−152.9	−68.0	−244.4	−24.3	−153.5	−69.9
	2	−210.2	−39.8	−158.4	−67.3	−246.6	−35.3	−155.7	−68.5
	3	−213.8	38.9	151.0	−175.7	−247.9	52.7	158.2	178.8
	4	−216.1	39.1	151.6	−177.0	−248.2	47.5	154.2	−178.3
	5	−200.2	51.6	162.1	174.9	−244.6	49.4	160.3	177.4
1z	1	−186.3	−54.0	−160.0	−73.1	−247.1	−51.0	−156.8	−71.2
	2	−184.7	−59.7	−164.1	−72.1	−250.0	−58.1	−162.3	−71.8
	3	−181.5	53.5	148.2	−178.0	−246.9	51.9	150.7	−178.4
	4	−180.6	64.6	139.0	−173.9	−245.0	63.9	141.7	−173.5
	5	−176.3	57.6	157.8	174.3	−245.8	51.6	156.0	176.5
	6	−177.9	54.4	148.4	−177.3	−246.4	53.1	153.1	179.3
1a	1	−221.3	−54.0	−153.9	−69.0	−343.8	−53.2	−158.7	−69.3
	2	−233.4	−55.2	−154.4	−69.3	−347.9	−58.6	−158.1	−73.9
	3	−237.4	−61.0	−151.5	−77.8	−347.8	−58.5	−157.7	−73.8
	4	−234.3	59.9	148.3	179.6	−343.8	51.6	151.3	179.8
	5	−227.6	71.1	132.6	−174.2	−340.2	65.1	144.6	−177.7

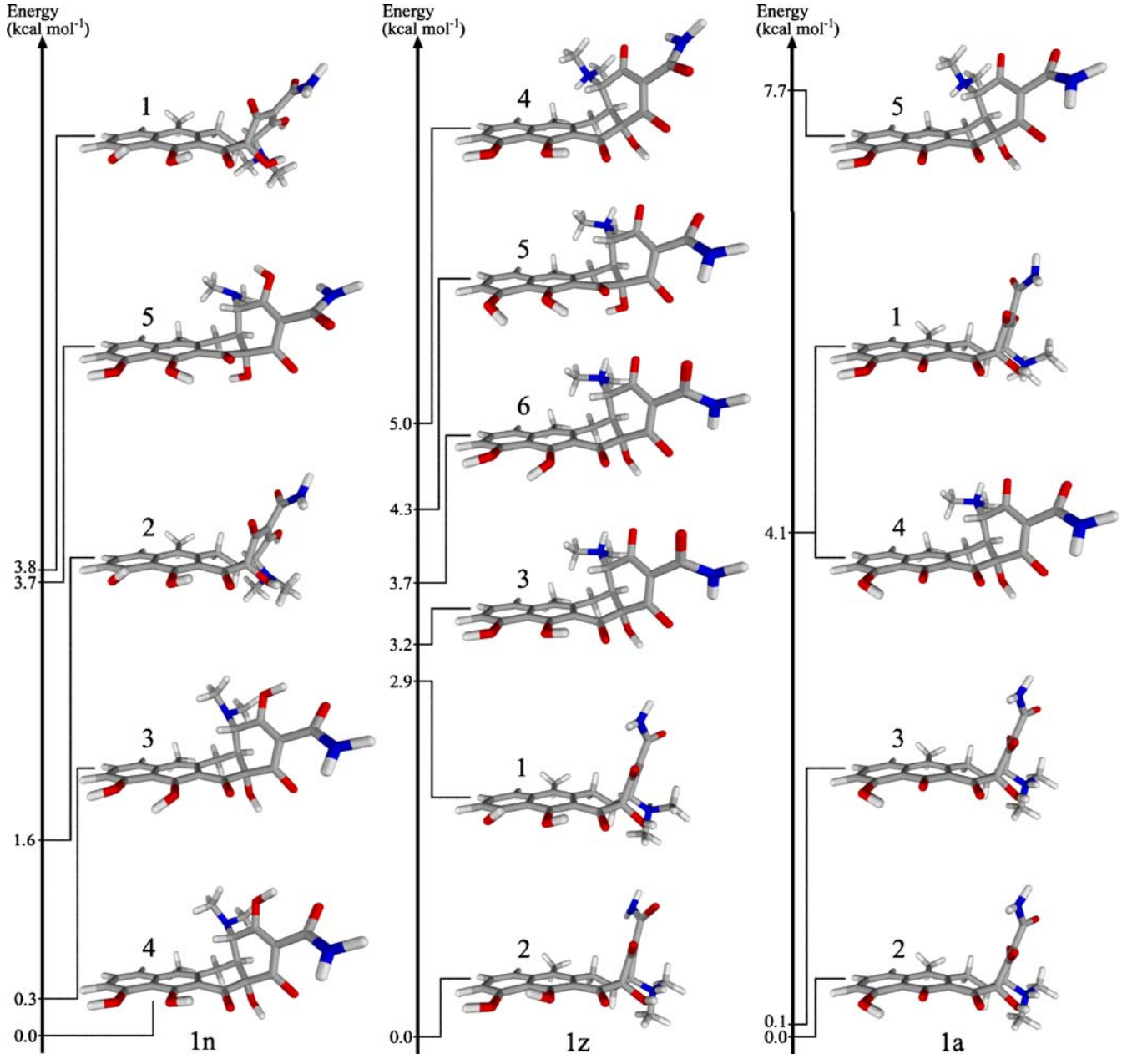

Fig. 2 Conformations and energy differences in solution for **1n**, **1z** and **1a**. The numbers indicate the different conformations and are consistent for Table 1 and Figs. 1, 2 and 3

mainly through the rotation of the OH-, amine- and amide groups, but some small differences in the distortion of ring A can be seen for both conformations. As zwitterionic structures are strongly disfavored in the gas phase, the minimum of **1n** is 29.8 kcal mol^{-1} more stable than **1z**. Because of different charges and the deprotonation states, no energy comparison of **1a** with **1n** or **1z** is possible.

Including solvent effects by COSMO only resulted in small structural changes. The conformation **T** for **1n** and **E** for **1z** and **1a** for the absolute minima are retained, but are represented by different conformers than in the gas phase for **1z** and **1a**, as shown in Fig. 2. The energy differences between the two conformations are 1.6 kcal mol^{-1} for **1n**, 3.2 kcal mol^{-1} for **1z** and 4.1 kcal mol^{-1} for **1a**.

Magnesium surface scan

Magnesium-interaction positions within a 15 kcal mol^{-1} range above the absolute minimum of the same total formula are shown in Fig. 3. Because of the special attention paid to masked interaction positions, the optimized structure for each magnesium position within one conformation can differ only in the rotation of acidic hydrogen atoms [11]. For clarity, these acidic hydrogen atoms are shown in the conformation obtained for the absolute minimum of the protonation state/conformation. Almost every absolute minimum is positioned in the vicinity of the region defined by O_1, N_{amide} and O_3, with the exception of the *extended* **1a** conformations, where

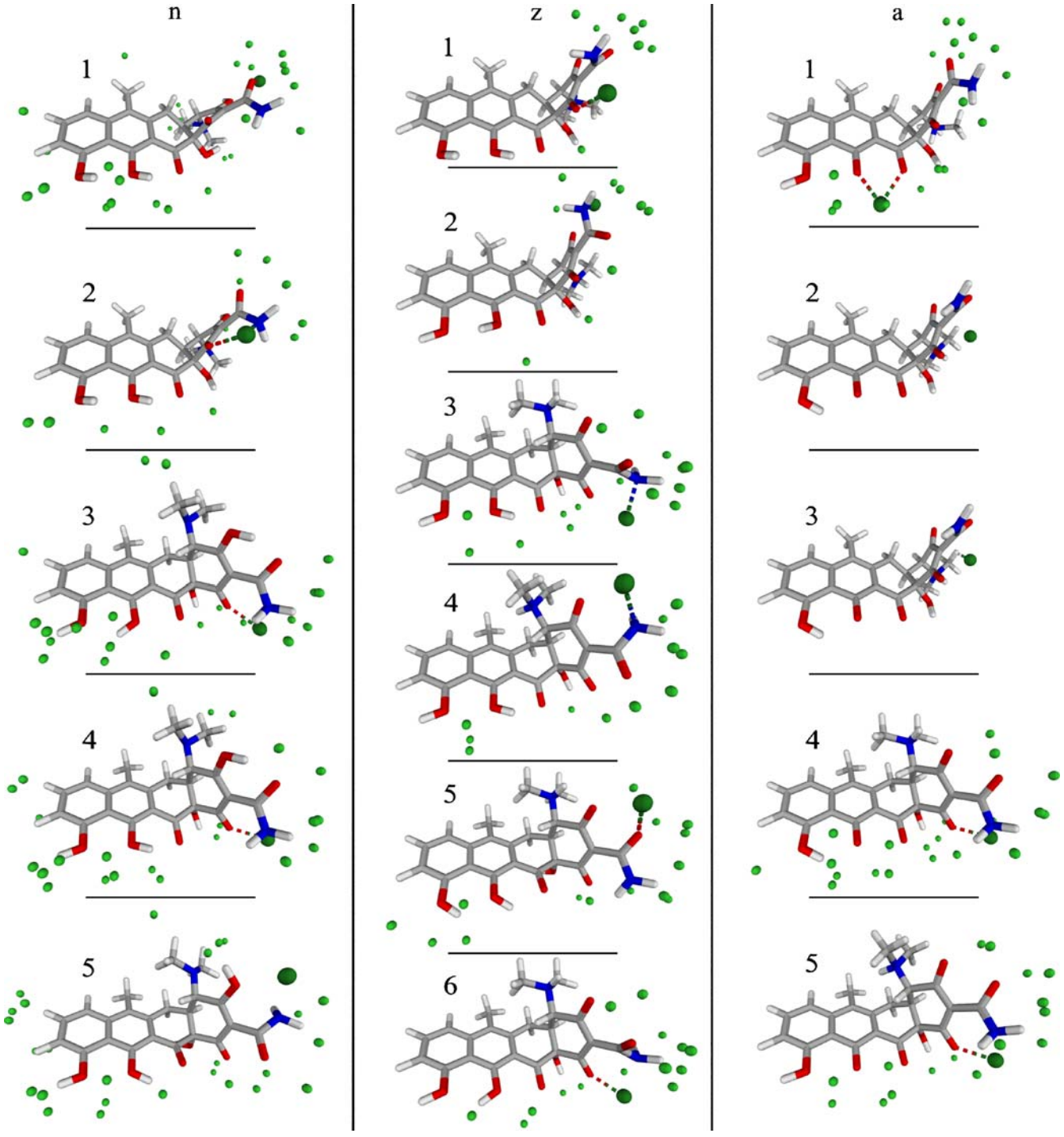

Fig. 3 Magnesium interaction points (*green*) for the different protonation states and conformers. The magnesium position for the absolute minimum of each cluster is distinguished by a *darker shade of green* and a *larger sphere radius*. Bonds between magnesium and **1** are indicated with *dashed lines*. The acidic hydrogen atoms are shown in the position present in the absolute minimum. The numbers indicate the different conformations and are consistent for Table 1 and Figs. 1, 2 and 3

magnesium is either bound to the amine group, causing an extreme energy minimum, or positioned between O_{11} and O_{12}, resembling the position taken in the active site of TetR. Less stable interaction positions are found for every other electronegative atom in **1**. For **1n**, additional magnesium positions interacting with the aromatic π-system and even the methyl group of C_6 are found.

Magnesium–5a,6–anhydrotetracycline complexes

Additionally to the pure magnesium complexes of **1**, water complexation spheres were created for the magnesium ions for each of the structures detected above by the surface scan. The magnesium ions were complexed with both four and five water molecules using predefined geometrical

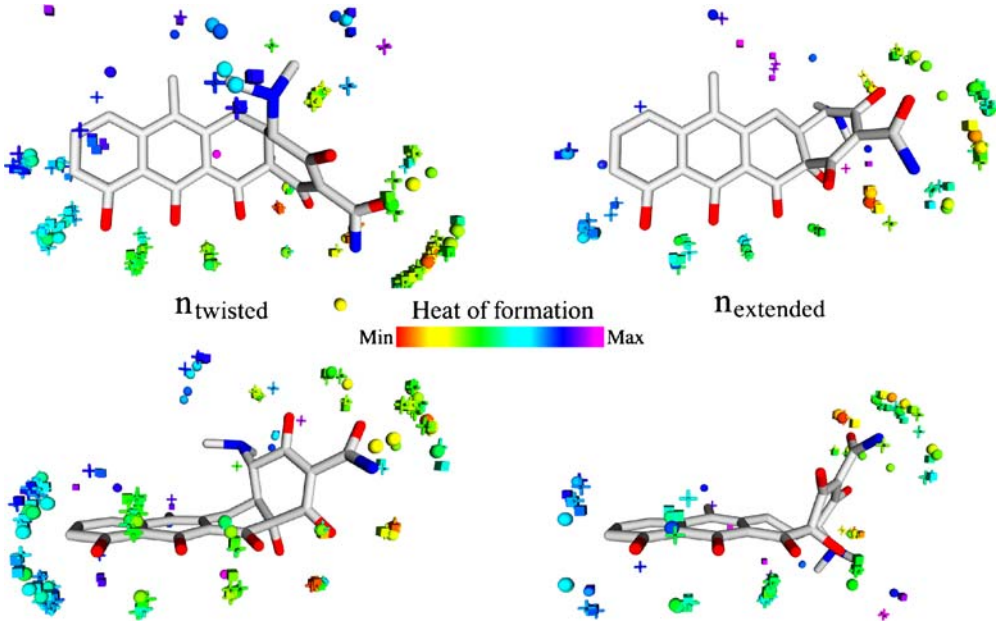

Fig. 4 Calculated magnesium ion positions for **1n** projected onto the cluster centers for the *twisted* (*left*) and *extended* (*right*) conformation. The *upper half* depicts the structures in *top view*, while the *lower half* gives their *side view*. The magnesium positions are colored by their heat of formation relative to the minimum for the corresponding total formulae and distinguish by their form between the complexes with zero (*sphere*), four (*box*) and five (*cross*) explicit water molecules. For clarity, all hydrogen atoms are omitted

fragments (see [11] for details) and were then optimized fully with AM1/COSMO. This approach yields three structures that differ by their water complexation spheres for each magnesium interaction position. The resulting 771 geometries (the total for the three protonation states) were clustered by the scaffold conformation of the carbon ring atoms, yielding the known conformations **T** and **E** shown in Figs. 4, 5 and 6 for **1n**, **1z** and **1a**, respectively. **1n** prefers **T** for all water-complexation spheres with an energy difference to the *extended* conformation of 1.4, 3.4 and 3.1 kcal mol^{-1} for zero, four and five water molecules, respectively (Table 2). Low-energy magnesium-ion positions are centered between O_1, O_3 and the amide group for complexes with conformation **E**, whereas for conformation **T** different areas are preferred by the pure complexes and the complexes with explicit water. The pure

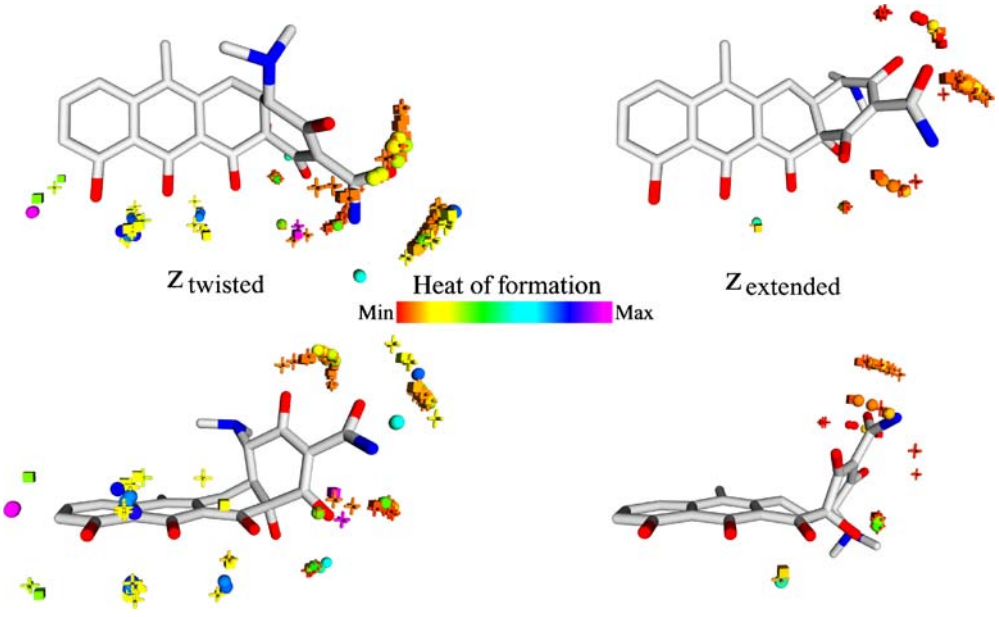

Fig. 5 Calculated magnesium ion positions for **1z** projected onto the cluster centers for the *twisted* (*left*) and *extended* (*right*) conformation. The *upper half* depicts the structures in *top view*, while the *lower half* gives their *side view*. The magnesium positions are colored by their heat of formation relative to the minimum for the corresponding total formulae and distinguish by their form between the complexes with zero (*sphere*), four (*box*) and five (*cross*) explicit water molecules. For clarity, all hydrogen atoms are omitted

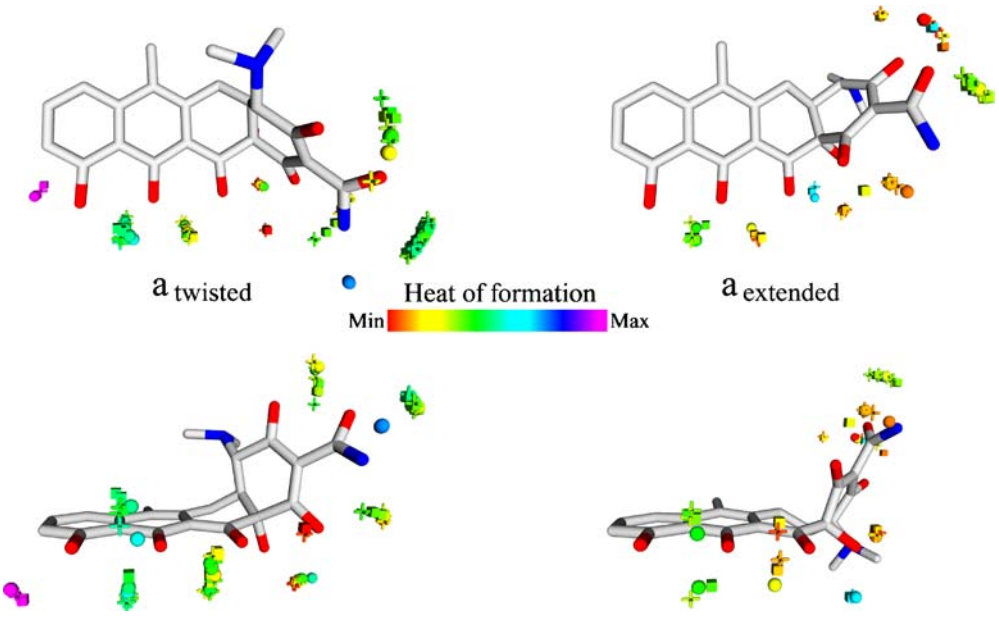

Fig. 6 Calculated magnesium ion positions for **1a** projected onto the cluster centers for the *twisted* (*left*) and *extended* (*right*) conformation. The *upper half* depicts the structures in *top view*, while the *lower half* gives their *side view*. The magnesium positions are colored by their heat of formation relative to the minimum for the corresponding total formulae and distinguish by their form between the complexes with zero (*sphere*), four (*box*) and five (*cross*) explicit water molecules. For clarity, all hydrogen atoms are omitted

complexes prefer direct amide binding, while the water complexes prefer O_1 as the interaction partner for the metal ion. A wider variety of magnesium ion positions is found for **1n** than for **1z** and **1a**. Unlike **1n**, **1z** prefers **E** by 3.9, 1.4 and 1.6 kcal mol^{-1} for zero, four and five water molecules, respectively, (Table 2), with a high density of magnesium ion positions between O_3 and the amide group. The *extended* **1z** clearly prefers magnesium ion positions at ring A, with only one exception for each protonation sphere in which magnesium binds to O_{11} and O_{12}, whereas the *twisted* conformation also exhibits magnesium ion positions near O_{10}, O_{11} and O_{12}. In comparison to **1n,** these ion positions are energetically closer to the absolute minimum for explicit water complexation spheres, and farther away for the pure magnesium complex. The *twisted* conformation differs analogously to **1n** between pure and explicit water complexes, but this time exhibits low-energy interactions with the explicit water complexes in the complete area defined by O_1, O_3 and the amide group and no real low-energy structures for pure complexes in conformation **T**. **1a** shows mixed behavior for the conformation of the absolute minimum for each complexation sphere. Pure magnesium complexes prefer the *extended* conformation **E** over **T** by 2.9 kcal mol^{-1}, while the water complexes prefer conformation **T** by 1.2 kcal mol^{-1} and 0.7 kcal mol^{-1} for four and five water molecules, respectively (Table 2). The interaction positions of the absolute minima for the complexes with explicit water are located between O_{12} and O_1, while the minimum of the pure magnesium complexes lies between O_3 and the amide group. Direct magnesium binding to the amide group is unfavorable and the areas around the absolute minima are preferred. One low-energy conformation with five water molecules in the *extended* conformation can be observed. Geometry data for the minima of each total formula in both conformations are given in the supplementary material.

Table 2 Conformation population and minimum energy for the different total formulae

Protonation	Water	Twisted conformation		Extended Conformation	
		Structures	Minimum energy (kcal mol^{-1})	Structures	Minimum energy (kcal mol^{-1})
1n	0	**77**	**−77.9**	42	−76.5
	4	**77**	**−411.8**	42	−408.4
	5	**77**	**−495.3**	42	−492.2
1z	0	61	−81.5	**19**	**−85.4**
	4	61	−415.4	**19**	**−416.8**
	5	61	−496.7	**19**	**−498.3**
1a	0	38	−179.6	**20**	**−182.5**
	4	**38**	**−516.8**	20	−515.6
	5	**38**	**−597.1**	20	−596.4

Bold numbers indicate the conformation of the absolute minimum

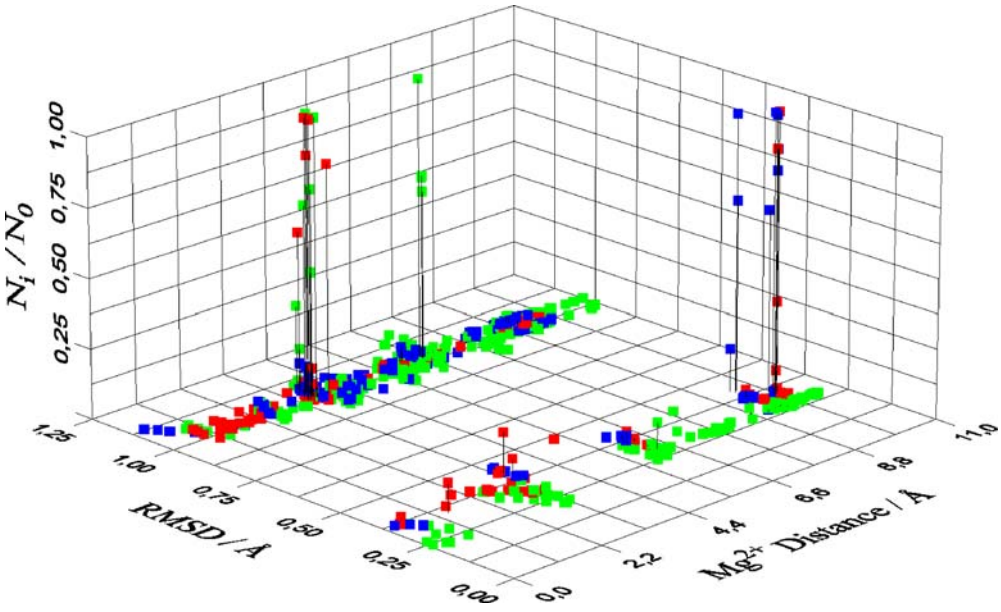

Fig. 7 Boltzmann population depending on the RMSD and the Mg^{2+} distances to the X-ray geometry of induced tetracycline. **1n** is colored *green*, **1z** *blue*, and **1a** *red*

Calculated Boltzmann populations

Boltzmann populations were calculated for each set of isomeric structures using the calculated heat of formation in water at 298 K. Fig. 7 shows the resulting populations plotted on a grid whose axes are the distance between the magnesium positions and the heavy-atom RMSD compared to the X-ray structure of tetracycline in the binding site of TetR [23]. The plot is clearly divided along the RMSD axis, separating the conformation **E** with low RMSD values and conformation **T**. Along the magnesium-distance axis, three significantly populated distances at about 3.5, 6.5 and 10 Å can be identified. The **1a** structure with five water molecules in *extended* conformation **E** described above shows a population proportion N_i/N_0 of 11%, a magnesium position distance of 1.3 Å and a RMSD of 0.3 Å. Only **1a** with a five water complexation sphere yields populated conformations this close to the X-ray structure of tetracycline in the binding site of TetR.

Hydrogen-bond network

The hydrogen-bond acceptor for $O_{12a}H$ indicates the conformation of the structure. O_1 as acceptor is indicative of conformation **T** and is bonded in 345 structures (65% of all possible structures), while the acceptor O_{12} indicates conformation **E** and is bonded in 139 structures (57%). Another parallel between the complexes with and without magnesium is the acceptor for the protonated amine in **1z** and **1a** as another indicator for the favored conformation. The acceptor O_{12a}, participating in 90 (77%) structures, indicates **E** and acceptor O_3, participating in 204 (69%) structures, indicates **T**. This classification is correct with only one exception each for $O_{12a}H$–O_{12} and N_{amine}–O_3. As the magnesium ion easily reorders and inserts into hydrogen bonds, no further specific hydrogen bond interactions could be observed.

Discussion

As **1** binds 500 times more strongly to TetR than **2** and induction without magnesium is observed for **1** [5], all differences in their conformations and magnesium complexes are important for understanding TetR induction. We therefore focus our discussion on the differences between the results for **1**, presented above, and those found previously for **2** [8–11].

The *extended* conformation **E** is more stable for all protonation patterns investigated previously for **2** and its magnesium complexes, [8–11] whereas unionized 5a,6–anhydrotetracycline **1n** shows a preference of the *twisted* conformation in the gas phase, in solvent and in complex with magnesium. **1z** and **1a** show an analogous behavior to **2** in the gas phase and in solvent, but the magnesium complexes of **1a** are very sensitive to explicit water complexation and only the complex without an explicit water complexation sphere exhibits conformation **E**. Other theoretical studies of **1** indicate the *extended* conformation to be preferred for **1z** [25], while for **1a** the two conformations are energetically nearly identical with a slight preference of the *extended* conformation [26]. As expected, the stiffening of ring B reduced the number of conformations found for **1**, but the preference of different conformations and the sensitivity to water complexation results in an even more complex conformational behavior than for **2**.

The magnesium ion positions identified are very similar for the two compounds, but **1** shows a greater density at ring A, while for **2** the O_{10}, O_{11} and O_{12}-regions are more highly populated, especially in the case of conformation **E**.

Theoretical studies of the interaction of **1z** and **1a** with aluminum [27] and zinc ions [28] identify for **1z** the O_3-amide and for **1a** the O_{11}–O_{12} as binding sites. The O_{11}–O_{12} and O_1–N_{amide} regions are found for zinc with **1a**. These regions are also important for the magnesium ion, but there are additional interaction sites as O_{amide}–N_{amide} for **1z** and O_3–O_{amide} for **1a**. Furthermore the interaction sites are not clearly differentiated by their energies.

No conformational change induced by addition of a magnesium ion or the water complexation sphere occurred. Of the 257 starting triplets, composed of one magnesium ion position with zero, four and five water molecules each, only 5% differed more than 2 Å in the optimized magnesium position, showing nearly no influence of the water complexation sphere on the final magnesium position but, as can be seen by the color coding of the magnesium ions within confined areas in Fig. 4, on the resulting heat of formation. A prominent example is the area around O_{10}, O_{11} and O_{12} in conformation **T** of **1z**, with energies in the lower third region for complexes with explicit water present and in the upper third for pure magnesium complexes. For **2** the mobility of starting triplets was 30% [11].

Comparison of the Boltzmann population between **1** and **2** shows significant differences for the conformations. For **2**, only *extended* conformations are significantly populated, whereas the conformation of **1** strongly depends on the protonation pattern and water complexation. Also no differentiation within the *twisted* conformation **T** between protonated and deprotonated N_{amine}, as exhibited for **2**, exists and large deviations in the magnesium position compared to the TetR X-ray structure for conformation **E** in **1** are preferred. **1** and **2** have low-energy, zwitteranionic structures with five water complexation spheres that resemble the X-ray structure of the tetracycline magnesium complex in the binding site of TetR strongly in common.

Conclusions

We have shown similarities and differences in the conformations of 5a,6–anhydrotetracycline **1** and tetracycline **2** and their magnesium complexes. Instead of the expected stiffening of the scaffold by dehydration and simplification of the structural diversity, our results suggest that **1**, while actual only exhibiting the *twisted* **T** and the *extended* **E** conformations, is far more complex than **2**, as the equilibrium between the conformations with and without magnesium complexation is very sensitive to environmental influences. Additionally, widespread magnesium complexation sites were identified for the different protonation patterns/water complexation spheres. These differences and similarities may play a role in determining the experimentally observed differences in their abilities to bind to the TetR dimer. Therefore, the results of this study will be used as a starting point for more accurate and more focused DFT calculations.

Acknowledgement We thank the Deutsche Forschungsgemeinschaft (Collaborative Research Center 473: *Mechanisms of Transcriptional Regulation*, Research Training Group 805/1: *Protein–Protein Interactions*) for financial support.

Appendix

Supporting Information Available

Dihedral angles and their boundaries used for clustering the "hot" structures obtained by molecular dynamics simulation. Geometric data for the minima of the 5a,6–anhydrotetracyline: magnesium complexes for each cluster/protonation pattern/water complexation sphere.

References

1. Chopra I, Roberts M (2001) Microbiol Mol Biol R 65:232–260
2. Hinrichs W, Orth P, Kisker C, Schnappinger D, Hillen W, Saenger W (1999) NATO Science Series, Series C: Mathematical and Physical Sciences 519:349–365
3. Hillen W, Berens C (2002) BIOspektrum 8:355–358
4. Hasan T, Allen M, Cooperman BS (1985) J Org Chem 50:1755–1757
5. Scholz O, Schubert P, Kintrup M, Hillen W (2000) Biochemistry 39:10914–10920
6. Takahashi M, Altschmied L, Hillen W (1986) J Mol Bio 187:341–348
7. Mitscher LA, Bonacci AC, Sokoloski TD (1968) Tetrahedron Lett 9:5361–5364
8. Lanig H, Gottschalk M, Schneider S, Clark T (1999) J Mol Model 5:46–62
9. Othersen OG, Beierlein F, Lanig H, Clark T (2003) J Phys Chem B 107:13743–13749
10. Othersen OG, Lanig H, Clark T (2006) J Phys Chem B (in preparation)
11. Othersen OG, Lanig H, Clark T (2003) J Med Chem 46:5571–5574
12. Machado FC, Demicheli C, Garnier-Suillerot A, Beraldo H (1995) J Inorg Biochem 60:163–173
13. Cosentino U, Vari RM, Saracino GAA, Pitea D, Moro G, Salmona M (2005) J Mol Model 11:17–25
14. Petrov AS, George R, Lamm G (2004) J Phys Chem B 108:6072–6081
15. Case DA, Pearlman DA, Caldwell JW, Cheatham III TE, Ross WS, Simmerling CL, Darden TA, Merz Jr KM, Stanton RV, Cheng AL, Vincent JJ, Crowley M, Ferguson DM, Radmer RJ, Seibel GL, Singh UC, Weiner PK, Kollman PA (1997) AMBER 5. University of California, San Francisco
16. Cornell WD, Cieplak P, Bayly C, Gould IR, Merz Jr KM, Ferguson DM, Spellmeyer DC, Fox T, Caldwell JW, Kollman PA (1995) J Am Chem Soc 117:5179–5197
17. Clark T, Alex A, Beck B, Burkhardt F, Chandrasekhar J, Gedeck P, Horn AHC, Hutter M, Martin B, Rauhut G, Sauer W, Schindler T, Steinke T (2003) Vamp, 9.0. Erlangen
18. Dewar MJS, Zoebisch EG, Healy EF, Stewart JJP (1985) J Am Chem Soc 107:3902–3909
19. Hutter MC, Reimers JR, Hush NS (1998) J Phys Chem B 102:8080–8090
20. Klamt A, Schüürmann G (1993) J Chem Soc Perk T 2:799–805
21. Grassy G, Blaney F, Bradshaw J, Huxley P, Lahana R, Snarey M (2000) Tsar 3.3. Oxford
22. Ward JH (1963) JASA 58:236–244

23. Protein Data Bank, http://www.rcsb.org/pdb
24. Heisterberg D, Labanowski J (1992) Quatfit. Columbus, Ohio; http://www.ccl.net/cca/software/SOURCES/C/quaternion-mol-fit/index.shtml
25. Dos Santos HF, de Almeida WB, Zerner MC (1998) J Pharm Sci 87:190–195
26. Dos Santos HF, Nascimento Jr CS, Belletato P, de Almeida WB (2003) J Mol Struct (Theochem) 626:305–319
27. de Almeida WB, Dos Santos HF, Zerner MC (1998) J Pharm Sci 87:1101–1108
28. de Almeida WB, Dos Santos HF, Rocha WR, Zerner MC (1998) J Chem Soc, Dalton Trans 15:2531–2536